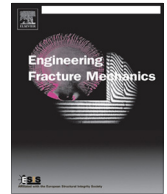




ELSEVIER

Contents lists available at ScienceDirect

Engineering Fracture Mechanics

journal homepage: www.elsevier.com/locate/engfracmech

Technical Note

On the displacement discontinuity method and the boundary element method for solving 3-D crack problems

Yijun Liu ^{*}

Mechanical Engineering, University of Cincinnati, P.O. Box 210072, Cincinnati, OH 45221-0072, USA

Institute for Computational Mechanics and Its Applications, Northwestern Polytechnical University, Xi'an, Shaanxi 710072, China

ARTICLE INFO

Article history:

Received 1 July 2016

Accepted 20 July 2016

Available online 8 August 2016

Keywords:

Displacement discontinuity method

Boundary element method

Equivalence

3-D crack problems

ABSTRACT

In this paper, it is shown that the equations of the displacement discontinuity method (DDM) for solving 3-D crack problems are exactly the same as the equations of the boundary element method (BEM) based on the boundary integral equation (BIE). Therefore, many of the results in the BEM research can be applied directly to the DDM, such as the results of analytical integration and fast solution methods, due to this equivalence or connection. A couple of examples are presented to show the accuracy of the DDM or the BEM with constant triangular elements in solving 3-D problems, when the analytical integration results are applied. It is concluded that the DDM can be applied to solve more complicated 3-D crack problems, such as interaction of multiple cracks and cracks with curved surfaces, with high accuracy and efficiency if the techniques available in the BEM are adopted.

© 2016 Elsevier Ltd. All rights reserved.

1. Introduction

The displacement discontinuity method (DDM) was proposed by Crouch in 1976 [1,2] for modeling cracks in elastic solids. Since then, many improvements and extensions of the DDM has been made (see, e.g., Refs. [3–12]). The DDM has been applied in many engineering fields, especially in rock mechanics [13], mining and petroleum engineering, including in modeling hydraulic fractures (e.g., [14–16]). In the original DDM, the displacement discontinuity across the two surfaces of a crack are assumed to be constant on line segments (for 2-D models) or area elements (for 3-D models) representing the crack. Displacement and stress fields in the cracked domain are related to the displacement discontinuities on the line segments or area elements by use of the elasticity solutions due to a point force or dislocation and the principle of superposition. A linear system of equations is formed directly that can be used to solve for the unknown displacement discontinuities on the crack surfaces. The method is easy to implement and accurate when the number of the line segments or area elements is sufficiently large [14,15]. To improve the accuracy of the DDM, higher-order representations of the displacement discontinuities can be applied [3,14,15]. However, there are still some unsettled questions with the DDM, especially for the 3-D cases. For example, numerical integration is still applied in the 3-D DDM for some of the integrals, even when constant elements are used [12]. Rectangular shaped elements are still used in modeling cracks with curved boundaries (e.g., a penny-shaped crack) that can only be represented by zigzagged boundaries [16]. In addition, the fast solution methods have only been applied to the 2-D DDM (e.g., [17–19]).

* Corresponding author at: Mechanical Engineering, University of Cincinnati, P.O. Box 210072, Cincinnati, OH 45221-0072, USA.

E-mail address: Yijun.Liu@uc.edu

The boundary element method (BEM) based on the elasticity boundary integral equation (BIE) [20] has been applied in solving crack problems for more than three decades [21–29]. There are many different approaches in the BEM for solving crack problems, including the multidomain BEM [24] using only the displacement (singular) BIE, BEM using the traction (hypersingular) BIE [25–34], or BEM using dual BIE formulations with various combinations of the displacement and traction BIEs [35–37]. With analytical integration for calculating the integrals in the BEM, accurate BEM results of the crack opening displacement (COD) and stress intensity factor (SIF) can be obtained with even constant elements [38–45]. With the help of the fast multiple method (FMM) [46–49] and the adaptive cross approximation (ACA) [50,51], large-scale BEM models with up to thousands of cracks or cracks in complicated mechanical parts can be solved successfully [39–41,52–55]. More comprehensive reviews of the BEM for solving crack problems can be found in Refs. [23,27,28,56].

There seem to be some connections and also some disconnections between the DDM and BEM research work. Both methods use the solution due to a point force or dislocation, the principle of superposition, and unknowns only on the boundary. Therefore, it is natural for researchers to link the two methods. In the literature, the DDM has been called a special indirect BEM, or similar to the direct BEM, or a third method based on physical arguments (e.g., [3,8,9,13–15]). Meanwhile, the research results regarding analytical integration, use of isoparametric elements with arbitrary triangular or quadrilateral shapes, and fast solution methods (FMM, ACA and others) used widely in the BEM are still not fully recognized in the DDM research. What is not clear, and also the reason of this work, is that the DDM can be shown to be equivalent to the BEM for solving crack problems. That is, the DDM not only can be called a BEM, but also is a subset of the BEM. Therefore, all the research results in the BEM can be, and should be, applied in the DDM to solve more complicated and large-scale crack problems.

Hong and Chen provided perhaps the earliest linkage between the 2-D DDM and BEM equations (see Refs. [25,57] for details). Linkov and Mogilevskaya [58,59] also noted that the DDM is equivalent to the BIE for 2-D crack problems and for 3-D cases [43,60]. Liu and Li [61] recently provided the direct proof of the equivalence of the 2-D DDM and BEM equations. They started with the traction BIE for a one-surface crack model, applied constant line elements and analytical integration results. They showed explicitly that the resulting BEM equations are exactly the same equations as given in the 2-D DDM [1]. In a recent comprehensive review article [62], Mogilevskaya also provided the proof of the equivalence of the 2-D DDM and BEM equations. However, to the author's best knowledge, no proof has been given in the literature to show that the 3-D DDM and BEM equations are identical for solving 3-D crack problems.

In this paper, it is shown explicitly that the discretization of the direct BIEs for a crack in a 3-D infinite elastic domain using constant elements will yield exactly the same equations as in the original 3-D DDM. Therefore, the DDM is indeed a BEM. With this connection, many of the results in the BEM can be applied to the DDM readily and many of the remaining issues with the DDM are in fact non-existent, such as analytical integration results, use of isoparametric elements, and fast solution methods. Even the DDM formulations can be simplified and the DDM equations can be written in a more compact form.

2. Equivalence of the DDM and BEM equations for 3-D crack problems

Consider a crack in a 3-D infinite elastic domain V (Fig. 1). The crack originally has two surfaces, S^+ (bottom surface) and S^- (top surface). In the DDM (and the BEM in this study), only one surface $S (=S^+)$ is used to represent the crack. The crack area is first assumed to be flat and its surface S is aligned with the 012 (*oxy*) plane (Fig. 1) in a local coordinate system 0123 (*oxyz*). For arbitrarily oriented and shaped cracks, additional transformations in the equations are needed for the DDM. However, there are no such assumptions and transformations needed in the BEM formulation.

Under the above mentioned conditions, the starting DDM equations for 3-D cases [2,6,12] can be written as follows (notation in Ref. [12] is used here):

$$\begin{cases} u_1(\mathbf{x}) = \frac{1}{8\pi(1-\nu)} \{ [2(1-\nu)I_3 - zI_{11}]D_1 - zI_{12}D_2 - [(1-2\nu)I_1 + zI_{13}]D_3 \}, \\ u_2(\mathbf{x}) = \frac{1}{8\pi(1-\nu)} \{ -zI_{12}D_1 + [2(1-\nu)I_3 - zI_{22}]D_2 - [(1-2\nu)I_2 + zI_{23}]D_3 \}, \\ u_3(\mathbf{x}) = \frac{1}{8\pi(1-\nu)} \{ [(1-2\nu)I_1 - zI_{13}]D_1 + [(1-2\nu)I_2 - zI_{23}]D_2 + [2(1-\nu)I_3 - zI_{33}]D_3 \}; \end{cases} \quad (1)$$

and

$$\begin{cases} \sigma_{11}(\mathbf{x}) = \frac{\mu}{4\pi(1-\nu)} \{ [2I_{13} - zI_{11}]D_1 + [2\nu I_{23} - zI_{12}]D_2 + [2\nu I_{33} - (1-2\nu)I_{11} - zI_{13}]D_3 \}, \\ \sigma_{22}(\mathbf{x}) = \frac{\mu}{4\pi(1-\nu)} \{ [2\nu I_{13} - zI_{22}]D_1 + [2I_{23} - zI_{22}]D_2 + [2\nu I_{33} - (1-2\nu)I_{22} - zI_{23}]D_3 \}, \\ \sigma_{33}(\mathbf{x}) = \frac{\mu}{4\pi(1-\nu)} \{ -zI_{13}D_1 - zI_{23}D_2 + [I_{33} - zI_{33}]D_3 \}, \\ \sigma_{12}(\mathbf{x}) = \frac{\mu}{4\pi(1-\nu)} \{ [(1-\nu)I_{23} - zI_{12}]D_1 + [(1-\nu)I_{13} - zI_{22}]D_2 - [(1-2\nu)I_{12} + zI_{123}]D_3 \}, \\ \sigma_{13}(\mathbf{x}) = \frac{\mu}{4\pi(1-\nu)} \{ [(1-\nu)I_{33} - \nu I_{11} - zI_{13}]D_1 - [\nu I_{12} + zI_{123}]D_2 - zI_{133}D_3 \}, \\ \sigma_{23}(\mathbf{x}) = \frac{\mu}{4\pi(1-\nu)} \{ -[\nu I_{12} + zI_{123}]D_1 + [(1-\nu)I_{33} - \nu I_{22} - zI_{223}]D_2 - zI_{233}D_3 \}; \end{cases} \quad (2)$$

where u_i and σ_{ij} (with $i, j = 1, 2, 3$) are the displacement and stress components, respectively, at point \mathbf{x} inside the domain, μ is the shear modulus, ν is Poisson's ratio, z is the third coordinate of point \mathbf{x} ($z = x_3$), and D_i is the displacement discontinuity on the crack surface S . To be consistent with the notation in DDM (Ref. [12]), the displacement discontinuity D_i is defined as

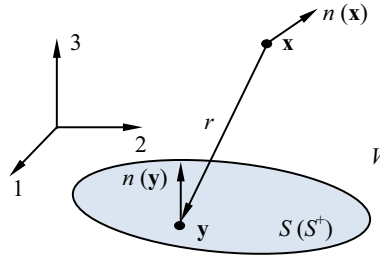


Fig. 1. A crack in an infinite 3-D elastic medium.

$$D_i(\mathbf{y}) = u_i(y_1, y_2, 0^+) - u_i(y_1, y_2, 0^-).$$

With this definition, D_1 is *negative* when the crack is pulled open (mode I case). The key functions denoted by I 's in expressions (1) and (2) are given by

$$\begin{cases} I = I(\mathbf{x}) = \int_A \frac{1}{r(\mathbf{x}, \mathbf{y})} dA(\mathbf{y}), \\ I_i = \frac{\partial I}{\partial x_i}, \quad I_{ij} = \frac{\partial^2 I}{\partial x_i \partial x_j}, \quad I_{ijk} = \frac{\partial^3 I}{\partial x_i \partial x_j \partial x_k}; \end{cases} \quad (3)$$

where r is the distance between \mathbf{x} (x_i , inside the domain) and \mathbf{y} (y_i , on the crack surface) and A is a typical contributing area on the crack surface S . It will be shown later on that Eqs. (1) and (2) can be written in more compact tensor forms.

In the DDM, the displacement and stress values are obtained by summing the contributions from each small area A (or element) on the crack surface S using Eqs. (1) and (2). To determine the unknown constant displacement discontinuity D_i on each small area A , the stress equations in (2) are applied on the crack surfaces where tractions are given, while the displacement equations in (1) are applied on surfaces where displacements are given. Details about the implementation of the DDM for 3-D crack problems can be found in the recent paper in Ref. [12].

To apply the BEM to solve the same crack problem shown in Fig. 1, we start with the following representation integral for the displacement field [20,29,49,63–65], assuming we still have two separate surfaces for the crack:

$$u_i(\mathbf{x}) = \int_{S^+ \cup S^-} [U_{ij}(\mathbf{x}, \mathbf{y}) t_j(\mathbf{y}) - T_{ij}(\mathbf{x}, \mathbf{y}) u_j(\mathbf{y})] dS(\mathbf{y}), \quad \forall \mathbf{x} \in V, \quad (4)$$

where \mathbf{x} and \mathbf{y} are called the source point and field point, respectively; u_i and t_i are the displacement and traction field, respectively; and U_{ij} and T_{ij} are the displacement and traction kernels in the Kelvin's solution, respectively [49].

The corresponding representation integral for the stress σ_{ij} or traction is [29,49,63–65]:

$$\sigma_{ij}(\mathbf{x}) n_j(\mathbf{x}) = \int_{S^+ \cup S^-} [K_{ij}(\mathbf{x}, \mathbf{y}) t_j(\mathbf{y}) - H_{ij}(\mathbf{x}, \mathbf{y}) u_j(\mathbf{y})] dS(\mathbf{y}), \quad \forall \mathbf{x} \in V, \quad (5)$$

where K_{ij} and H_{ij} are two new kernels in the Kelvin's solution [49]. For completeness, we list the expressions for the kernels (U , T , K and H) in the 3-D case in the following [49]:

$$U_{ij}(\mathbf{x}, \mathbf{y}) = \frac{1}{16\pi\mu(1-\nu)r} [(3-4\nu)\delta_{ij} + r_{,i}r_{,j}], \quad (6)$$

$$T_{ij}(\mathbf{x}, \mathbf{y}) = -\frac{1}{8\pi(1-\nu)r^2} \left\{ 3 \frac{\partial r}{\partial n} [(1-2\nu)\delta_{ij} + 3r_{,i}r_{,j}] - (1-2\nu)(r_{,i}n_j - r_{,j}n_i) \right\}, \quad (7)$$

$$K_{ij}(\mathbf{x}, \mathbf{y}) = \frac{1}{8\pi(1-\nu)r^2} [(1-2\nu)(\delta_{ij}r_{,k} + \delta_{jk}r_{,i} - \delta_{ik}r_{,j}) + 3r_{,i}r_{,j}r_{,k}] n_k(\mathbf{x}), \quad (8)$$

$$\begin{aligned} H_{ij}(\mathbf{x}, \mathbf{y}) = & \frac{\mu}{4\pi(1-\nu)r^3} \left\{ 3 \frac{\partial r}{\partial n} [(1-2\nu)\delta_{ik}r_{,j} + \nu(\delta_{ij}r_{,k} + \delta_{jk}r_{,i}) - 5r_{,i}r_{,j}r_{,k}] + 3\nu(n_i r_{,j} r_{,k} + n_k r_{,i} r_{,j}) \right. \\ & \left. - (1-4\nu)\delta_{ik}n_j + (1-2\nu)(3n_j r_{,i} r_{,k} + \delta_{ij}n_k + \delta_{jk}n_i) \right\} n_k(\mathbf{x}); \end{aligned} \quad (9)$$

in which r is the distance between source point \mathbf{x} and field point \mathbf{y} , $(\cdot)_{,i} = \partial(\cdot)/\partial y_i$, δ_{ij} is the Kronecker δ symbol, n_i is the direction cosine of the normal at \mathbf{y} , and $n_k(\mathbf{x})$ is a unit vector at field point \mathbf{x} .

When S^- is collapsed onto S^+ ($= S$) to form a one surface model for the crack (Fig. 1), the displacement integral (4) is reduced to the following equation [36,66]:

$$u_i(\mathbf{x}) = \int_S [U_{ij}(\mathbf{x}, \mathbf{y}) \Sigma t_j(\mathbf{y}) - T_{ij}(\mathbf{x}, \mathbf{y}) \Delta u_j(\mathbf{y})] dS(\mathbf{y}), \quad \forall \mathbf{x} \in V, \quad (10)$$

and the stress or traction integral (5) is reduced to the following equation [29,31–34,36,37]:

$$\sigma_{ij}(\mathbf{x})n_j(\mathbf{x}) = \int_S [K_{ij}(\mathbf{x}, \mathbf{y})\Sigma t_j(\mathbf{y}) - H_{ij}(\mathbf{x}, \mathbf{y})\Delta u_j(\mathbf{y})]dS(\mathbf{y}), \quad \forall \mathbf{x} \in V, \tag{11}$$

where $\Delta u_i = u_i|_{S^+} - u_i|_{S^-}$, $\Sigma u_i = u_i|_{S^+} + u_i|_{S^-}$, $\Delta t_i = t_i|_{S^+} - t_i|_{S^-}$, and $\Sigma t_i = t_i|_{S^+} + t_i|_{S^-}$. Assuming that the load on the crack surface is in equilibrium (such as a pressure load), including the traction free case, we have

$$\Sigma t_i = t_i|_{S^+} + t_i|_{S^-} = 0. \tag{12}$$

Thus displacement integral (10) is further reduced to:

$$u_i(\mathbf{x}) = - \int_S T_{ij}(\mathbf{x}, \mathbf{y})\Delta u_j(\mathbf{y})dS(\mathbf{y}), \quad \forall \mathbf{x} \in V, \tag{13}$$

and the stress or traction integral (11) is further reduced to:

$$\sigma_{ij}(\mathbf{x})n_j(\mathbf{x}) = - \int_S H_{ij}(\mathbf{x}, \mathbf{y})\Delta u_j(\mathbf{y})dS(\mathbf{y}), \quad \forall \mathbf{x} \in V. \tag{14}$$

It is clear that both the displacement and stress fields inside the elastic medium are solely determined by the displacement discontinuity across the crack surfaces. In the BEM, the BIEs based on Eqs. (13) and (14) are derived by letting the source point \mathbf{x} approach the boundary S .

We now show that the discretized form of Eq. (13) gives exactly the same results for the displacement field as given by the DDM equations in (1). First, Eq. (13) can be discretized as follows, using the concept of constant boundary elements [29,49,63–65]:

$$u_i(\mathbf{x}) = - \sum_e \int_{A_e} T_{ij}(\mathbf{x}, \mathbf{y})dA(\mathbf{y})\Delta u_j, \tag{15}$$

where A_e is the area of a typical element on which the displacement discontinuity Δu_j is assumed to be constant, and the summation is over all the elements used to discretize the crack surface S . Next, we note that the kernel T_{ij} in Eq. (7) can be rewritten in the following form:

$$T_{ij}(\mathbf{x}, \mathbf{y}) = - \frac{1}{8\pi(1-\nu)} \left\{ r_{,ijk}n_k - 2\nu \left(\frac{1}{r} \right)_{,i} n_j - 2(1-\nu) \left[\delta_{ij} \left(\frac{1}{r} \right)_{,k} n_k + \left(\frac{1}{r} \right)_{,j} n_i \right] \right\}, \tag{16}$$

and the following results:

$$\begin{cases} r_{,i} = \frac{y_i - x_i}{r}, & r_{,ij} = \frac{1}{r} (\delta_{ij} - r_{,i}r_{,j}), & r_{,ijk} = \frac{1}{r^2} (3r_{,i}r_{,j}r_{,k} - \delta_{ij}r_{,k} - \delta_{jk}r_{,i} - \delta_{ik}r_{,j}), \\ r_{,ijkl} = \frac{1}{r^3} [-15r_{,i}r_{,j}r_{,k}r_{,l} + 3(r_{,i}r_{,j}\delta_{kl} + r_{,i}r_{,k}\delta_{jl} + r_{,j}r_{,k}\delta_{il} + r_{,i}r_{,l}\delta_{jk} + r_{,j}r_{,l}\delta_{ik} + r_{,k}r_{,l}\delta_{ij}) - \delta_{ij}\delta_{kl} - \delta_{ik}\delta_{jl} - \delta_{jk}\delta_{il}], \\ \left(\frac{1}{r} \right)_{,i} = -\frac{1}{r^2} r_{,i}, & \left(\frac{1}{r} \right)_{,ij} = \frac{1}{r^3} (3r_{,i}r_{,j} - \delta_{ij}), & \left(\frac{1}{r} \right)_{,ijk} = \frac{3}{r^4} (-5r_{,i}r_{,j}r_{,k} + \delta_{ij}r_{,k} + \delta_{jk}r_{,i} + \delta_{ik}r_{,j}); \end{cases} \tag{17}$$

where $(\cdot)_{,i} = \partial(\cdot)/\partial y_i = -\partial(\cdot)/\partial x_i$. In the local coordinate system 0123 in Fig. 1, normal $n(\mathbf{y})$ is in the same direction as z -axis, that is, $n_k(\mathbf{y}) = \delta_{3k}$. Thus, in this special case, T_{ij} in Eq. (16) is further reduced to

$$T_{ij}(\mathbf{x}, \mathbf{y}) = - \frac{1}{8\pi(1-\nu)} \left\{ r_{,3ij} - 2\nu \delta_{3j} \left(\frac{1}{r} \right)_{,i} - 2(1-\nu) \left[\delta_{ij} \left(\frac{1}{r} \right)_{,3} + \delta_{3i} \left(\frac{1}{r} \right)_{,j} \right] \right\}. \tag{18}$$

Substituting this into Eq. (15) and applying results in Eqs. (3) and (17), we obtain

$$\begin{aligned} u_i(\mathbf{x}) &= \frac{1}{8\pi(1-\nu)} \sum_e \left[\int_{A_e} r_{,3ij}dA + 2\nu \delta_{3j}I_i + 2(1-\nu)(\delta_{ij}I_3 + \delta_{3i}I_j) \right] \Delta u_j \\ &= \frac{1}{8\pi(1-\nu)} \sum_e \left[\int_{A_e} \left(\frac{1}{r^2} (3r_{,i}r_{,j}r_{,3} - \delta_{ij}r_{,3} - \delta_{3j}r_{,i} - \delta_{3i}r_{,j}) \right) dA \Delta u_j + 2\nu I_i \Delta u_3 + 2(1-\nu)(I_3 \Delta u_i + \delta_{3i}I_j \Delta u_j) \right] \\ &= \frac{1}{8\pi(1-\nu)} \sum_e \left[\int_{A_e} \left(\frac{1}{r^3} (3r_{,i}r_{,j} - \delta_{ij})(rr_{,3}) - \frac{1}{r^2} (r_{,i}\delta_{3j} + r_{,j}\delta_{3i}) \right) dA \Delta u_j + 2\nu I_i \Delta u_3 + 2(1-\nu)(I_3 \Delta u_i + \delta_{3i}I_j \Delta u_j) \right] \\ &= \frac{1}{8\pi(1-\nu)} \sum_e [(I_{ij}(-z) - (\delta_{3j}I_i + \delta_{3i}I_j))\Delta u_j + 2\nu I_i \Delta u_3 + 2(1-\nu)(I_3 \Delta u_i + \delta_{3i}I_j \Delta u_j)], \end{aligned}$$

that is,

$$u_i(\mathbf{x}) = \frac{1}{8\pi(1-\nu)} \sum_e \{ 2(1-\nu)I_3 D_i + [(1-2\nu)\delta_{3i}I_j - zI_{ij}]D_j - (1-2\nu)I_i D_3 \}. \tag{19}$$

where $D_i = \Delta u_i$ (the displacement discontinuity). This is a compact and general expression for the displacement field based on the representation integral when constant elements are used. Letting $i = 1, 2, 3$ in Eq. (19), we obtain the following expressions for the three displacement components, respectively:

$$\begin{cases} u_1(\mathbf{x}) = \frac{1}{8\pi(1-\nu)} \sum_e \{ [2(1-\nu)I_3 - zI_{11}]D_1 - zI_{12}D_2 - [(1-2\nu)I_1 + zI_{13}]D_3 \}, \\ u_2(\mathbf{x}) = \frac{1}{8\pi(1-\nu)} \sum_e \{ -zI_{12}D_1 + [2(1-\nu)I_3 - zI_{22}]D_2 - [(1-2\nu)I_2 + zI_{23}]D_3 \}, \\ u_3(\mathbf{x}) = \frac{1}{8\pi(1-\nu)} \sum_e \{ [(1-2\nu)I_1 - zI_{13}]D_1 + [(1-2\nu)I_2 - zI_{23}]D_2 + [2(1-\nu)I_3 - zI_{33}]D_3 \}. \end{cases} \quad (20)$$

These are exactly the same results as the displacement components given by the DDM equations in (1) when they are summed over all the small contributing areas over the crack surface. That is, Eq. (19) from the BEM is identical to equations in Eq. (1).

To show that the stress field given by representation integral (14) is the same as that given by the DDM equations in (2), we first note that the H_{ij} kernel given in Eq. (9) can be rewritten as follows:

$$H_{ij}(\mathbf{x}, \mathbf{y}) = \frac{\mu}{4\pi(1-\nu)} \left\{ r_{,ijkl}n_l - 2\nu \left[\left(\frac{1}{r}\right)_{,ik} n_j + \left(\frac{1}{r}\right)_{,jl} n_i \delta_{ik} \right] - (1-\nu) \left[\left(\frac{1}{r}\right)_{,ij} n_k + \left(\frac{1}{r}\right)_{,jk} n_i + \left(\frac{1}{r}\right)_{,kl} n_l \delta_{ij} + \left(\frac{1}{r}\right)_{,il} n_l \delta_{jk} \right] \right\} n_k(\mathbf{x}), \quad (21)$$

in which the derivatives of r and its inverse are given in Eq. (17). In the local coordinate system (Fig. 1), we have $n_i = \delta_{3i}$. Replacing all the normal components within the curly bracket in the above equation with $n_i = \delta_{3i}$, we have

$$H_{ij}(\mathbf{x}, \mathbf{y}) = \frac{\mu}{4\pi(1-\nu)} \left\{ r_{,3ijk} - 2\nu \left[\left(\frac{1}{r}\right)_{,ik} \delta_{3j} + \left(\frac{1}{r}\right)_{,3j} \delta_{ik} \right] - (1-\nu) \left[\left(\frac{1}{r}\right)_{,ij} \delta_{3k} + \left(\frac{1}{r}\right)_{,jk} \delta_{3i} + \left(\frac{1}{r}\right)_{,3k} \delta_{ij} + \left(\frac{1}{r}\right)_{,3i} \delta_{jk} \right] \right\} n_k(\mathbf{x}), \quad (22)$$

Thus, the discretized equation of the stress integral (14) can be written as:

$$\begin{aligned} \sigma_{ij}n_j(\mathbf{x}) = & -\frac{\mu}{4\pi(1-\nu)} \sum_e \int_{A_e} \left\{ r_{,3ijk} - 2\nu \left[\left(\frac{1}{r}\right)_{,ik} \delta_{3j} + \left(\frac{1}{r}\right)_{,3j} \delta_{ik} \right] \right. \\ & \left. - \left(1-\nu\right) \left[\left(\frac{1}{r}\right)_{,ij} \delta_{3k} + \left(\frac{1}{r}\right)_{,jk} \delta_{3i} + \left(\frac{1}{r}\right)_{,3k} \delta_{ij} + \left(\frac{1}{r}\right)_{,3i} \delta_{jk} \right] \right\} dA n_k(\mathbf{x}) \Delta u_j. \end{aligned}$$

Applying the notations in Eq. (3) and relations in Eq. (17), we obtain

$$\sigma_{ij}n_j(\mathbf{x}) = \frac{\mu}{4\pi(1-\nu)} \sum_e [-zI_{ijk} - \nu(\delta_{3i}I_{jk} + \delta_{3j}I_{ik}) - (1-2\nu)\delta_{3j}I_{ik} + 2\nu\delta_{ik}I_{3j} + (1-\nu)(\delta_{ij}I_{3k} + \delta_{jk}I_{3i})] n_k(\mathbf{x}) D_j, \quad (23)$$

in which $D_j = \Delta u_j$ has been applied. This is the equation for stress or traction at \mathbf{x} on a plane with normal $n_j(\mathbf{x})$ (Fig. 1). To obtain the stress components at \mathbf{x} in all three coordinate directions, let $n_j(\mathbf{x}) = \delta_{mj}$, $n_k(\mathbf{x}) = \delta_{mk}$, with $m = 1, 2, 3$ (representing the three coordinate direction), respectively. Then, equation (23) yields the following expression for the general stress components:

$$\sigma_{ij}(\mathbf{x}) = \frac{\mu}{4\pi(1-\nu)} \sum_e [-zI_{ijk} - \nu(\delta_{3i}I_{jk} + \delta_{3j}I_{ik}) - (1-2\nu)\delta_{3k}I_{ij} + 2\nu\delta_{ij}I_{3k} + (1-\nu)(\delta_{ik}I_{3j} + \delta_{jk}I_{3i})] D_k, \quad (24)$$

after changing the free and dummy indices. Similar to the expression for displacement, this compact expression for stress can be shown to give exactly the same six expressions for all the stress components as those in Eq. (2) for the DDM when the contributions from all small areas are added up.

Therefore, the equivalence of the DDM and BEM for solving 3-D crack problems has been established explicitly here using the representation integrals for the displacement and stress fields which are discretized with constant elements.

3. Analytical integration results for the 3-D DDM and BEM

The analytical integration results for all the integrals defined in Eq. (3) and used in DDM Eqs. (1) and (2) are given by Kuriyama, et al. in Ref. [6]. The expressions are very lengthy, especially for those for the derivatives of function I . It was pointed out that the expressions given in Ref. [6] can yield infinite values in calculation when the field point \mathbf{x} is located on any extension line of an edge of the triangular element on which integration is performed [12]. Therefore, numerical integration schemes are still applied in some cases in order to avoid this instability problem in the work in Ref. [12]. These approaches seem to be not very efficient as the analytical expressions in Ref. [6] are very lengthy, or may not be accurate if numerical integration is still used for some of the integrals as in Ref. [12].

Since we have proved the equivalence of the 3-D DDM and BEM equations, the analytical integration results in the BEM can be applied directly to the 3-D DDM case. In the BEM, instead of integrating the I function and its derivatives in Eq. (3) one by one directly, the kernel functions (U , T , K , and H) are integrated analytically on each element. Because the kernel functions are combinations of the I function and its derivatives as shown earlier, the analytical integration results in the BEM are more compact compared to those for the DDM [6]. This can render better computational efficiency when the BEM analytical integration results are applied. In addition, the infinite value problem in the DDM integration results as mentioned in Ref. [12] are not present for those integration results in the BEM. Thus, the analytical integration results in the BEM are also more robust. No numerical integration is needed at all in the BEM when constant elements are used. Complete results of analytical integration results in the 3-D BEM on triangular and quadrilateral constant and linear elements, and special cases of quadratic elements, can be found in, e.g., Refs. [38,43–45,67–70] and the references therein.

The 3-D BEM analytical integration results mentioned above can be applied to the 3-D DDM directly to improve its efficiency and accuracy. For constant elements in either triangular or quadrilateral shapes, we apply the analytical integration results reported by Fukui in Ref. [38] in our BEM code. The analytical integration formulas in Ref. [38] are straightforward, compact, numerically stable and efficient in computing, especially in solving large-scale 3-D elastostatic problems [39–41,49,71,72].

4. Numerical examples

The BEM with constant elements has been considered not adequate for solving stress concentration and singularity problems, due to the piecewise constant displacement and traction fields assumed on the boundary. On the other hand, the DDM has been used for decades in solving crack related problems with reasonable results. Due to the connection of the BEM and DDM, the use of constant elements in the BEM need to be reevaluated. In this section, we will show that good BEM (or DDM) results for modeling 3-D problems can be obtained with constant elements if the analytical integration results are applied and finer meshes are used in the discretization. Other examples of using constant elements in the BEM can be found in Refs. [39–42,49,71–73].

Two examples are given in the following to show the effectiveness of the BEM with constant triangular elements in solving a 3-D stress concentration problem and a crack problem. The analytical integration formulas in Ref. [38] are used for all integrals in the BIEs.

4.1. The spherical void problem

The stress concentration problem of a spherical void in an infinite 3-D elastic domain is analyzed by the BEM. The void is centered at the origin and has a radius a . The void surface is traction free and a remote uniform stress σ_∞ is applied in the z -direction. The analytical solution of the maximum radial displacement on the void surface is given by (e.g., [74]):

$$u_{\max} = u_3(0, 0, a) = \frac{3\sigma_\infty a (1 - \nu)(9 + 5\nu)}{2E (7 - 5\nu)}, \quad (25)$$

where E is Young's modulus. The analytical solution of the maximum hoop stress is given by [75]:

$$\sigma_{\max} = \sigma_{33}(x, y, 0) = \frac{27 - 15\nu}{2(7 - 5\nu)} \sigma_\infty. \quad (26)$$

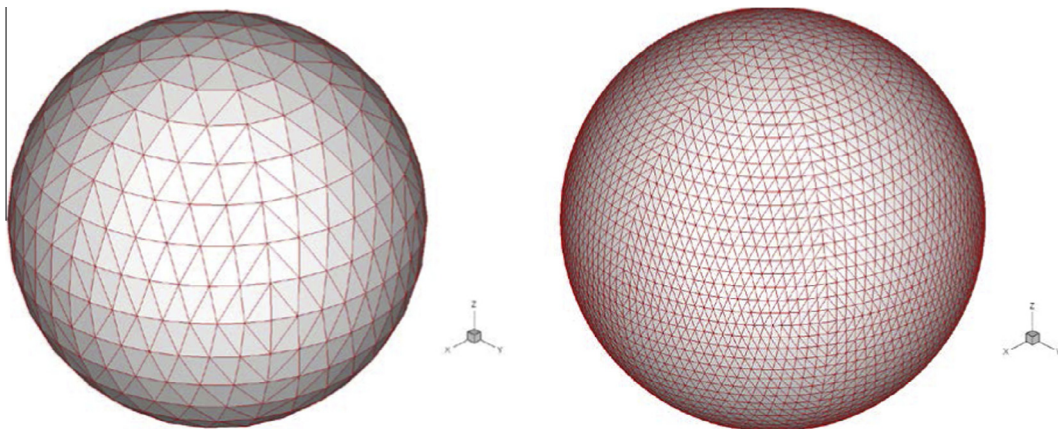


Fig. 2. Two BEM models used for modeling the spherical void with the number of elements $M = 768$ (left) and $M = 6912$ (right).

The displacement BIE (CBIE) and the so called dual BIE (a linear combination of the displacement BIE and the traction BIE) are used in the BEM solutions. The traction BIE cannot be applied alone to solve this type of problems since it has nonunique displacement solutions on the surfaces of a void [76]. The constants used for this example are: Young’s modulus $E = 1$, Poisson’s ratio $\nu = 0.3$, radius $a = 1$, and remote stress $\sigma_\infty = 1$. Five BEM models with the total number of elements (M) = 768, 1728, 3072, 4800, and 6912 are used in the computation. Two BEM models used are shown in Fig. 2.

Contour plots of the displacement u_3 and stress σ_{33} for the finest mesh ($M = 6912$) are shown in Fig. 3. Tables 1 and 2 summarize the results of the maximum radial displacement and hoop stress, respectively. It is shown in Table 1 that the displacement results converge to the exact solution very quickly and monotonically, with the CBIE providing slightly better results than the dual BIE. Both the CBIE and dual BIE displacement results with the finest mesh ($M = 6912$) have an error within 0.5%. The stress results in Table 2 converge to the exact solution slower than the displacement results, with the CBIE giving better results than the dual BIE. The CBIE stress results converge to within 0.5% of error, while the dual BIE stress results converge to 1.55% of error.

This example shows that with sufficiently fine mesh, the BEM with constant elements (or the DDM) can provide sufficiently accurate results in solving stress concentration problems. Another example of a spherical rigid inclusion in an infinite elastic medium solved by using the BEM with constant elements was reported in [72] where similarly accurate results were obtained.

4.2. The penny-shaped crack problem

A penny-shaped crack in an infinite 3-D elastic medium is considered next. The crack has a radius a and lies in the oxy plane. A remote load σ_∞ is applied in the z direction. The analytical solution of the crack opening displacement (COD) is given by [77]:

$$\text{COD} = 2w(x, y, 0) = \frac{4(1 - \nu)\sigma_\infty}{\pi\mu} \sqrt{a^2 - x^2 - y^2}. \tag{27}$$

The analytical solution of the stress intensity factor (SIF) is given by [78]:

$$K_I = \frac{2}{\pi} \sigma_\infty \sqrt{\pi a}. \tag{28}$$

To determine the SIF using the BEM, the following relation is applied [78]:

$$K_I = \frac{\mu}{4(1 - \nu)} \text{CTOD} \sqrt{\frac{2\pi}{r}}, \tag{29}$$

where r is the distance from the crack front to the point of evaluation, CTOD is the crack-tip opening displacement at the point of evaluation. In this study, this formula is applied at one point (on the first layer of elements from the crack front). Traction BIE (5) (with \mathbf{x} on the crack surface) is used in this case, which yields the COD directly after the solution.

The material constants for the infinite medium used are: Young’s modulus $E = 1$, and Poisson’s ratio $\nu = 0.25$. The crack is modeled with one surface that is discretized using seven meshes with the number of elements $M = 96, 384, 864, 1536, 2400, 3456,$ and 4704 , respectively. Two meshes ($M = 96$ and 2400) are shown in Fig. 4. The contour plots of the computed COD over the crack surface and SIF along the crack front line are shown in Fig. 5 for the mesh with $M = 2400$. The COD results along the positive x -axis is shown in Fig. 6 and good agreement between the BEM results and the analytical solution is

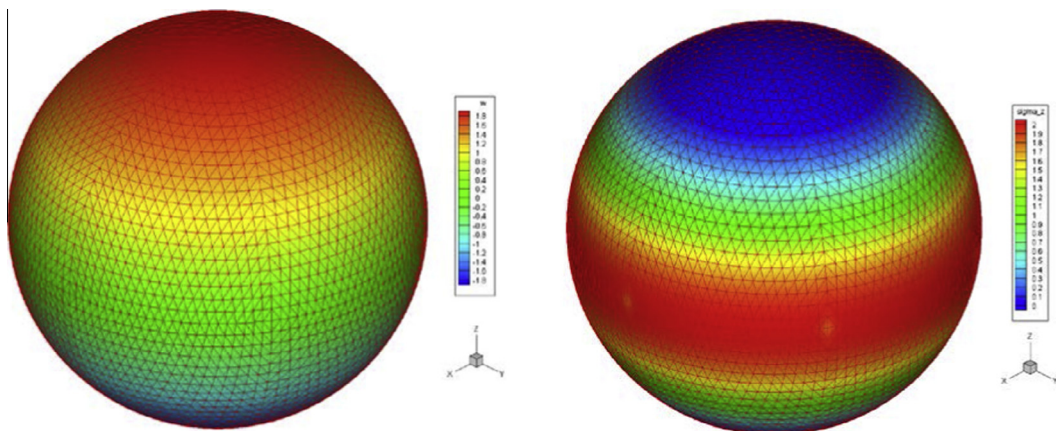


Fig. 3. Contour plots of the displacement u_3 (left) and stress σ_{33} (right) for the BEM model with $M = 6912$ and solved with the CBIE.

Table 1

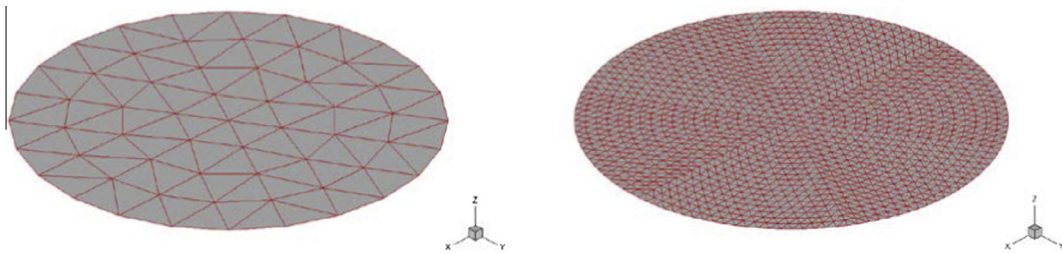
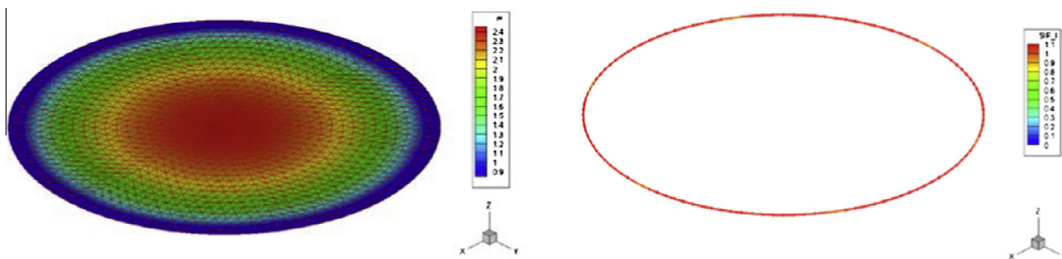
Results of maximum radial displacement.

No. of elements	Max. displacement ($\times \sigma_{\infty} a / E$)		Relative error	
	CBIE	Dual BIE	CBIE (%)	Dual BIE (%)
768	1.98165	1.97127	1.14	1.66
1728	1.99338	1.98654	0.56	0.90
3072	1.99771	1.99268	0.34	0.59
4800	1.99982	1.99586	0.24	0.43
6912	2.00102	1.99776	0.18	0.34
Analytical solution	2.00455		–	

Table 2

Results of maximum hoop stress.

No. of elements	Max. hoop stress ($\times \sigma_{\infty}$)		Relative error	
	CBIE	Dual BIE	CBIE (%)	Dual BIE (%)
768	1.98758	2.05807	2.83	0.62
1728	2.01710	2.07770	1.39	1.58
3072	2.02794	2.08019	0.86	1.70
4800	2.03320	2.07912	0.60	1.65
6912	2.03621	2.07723	0.45	1.55
Analytical solution	2.04545		–	

**Fig. 4.** Two BEM models used for modeling the penny-shaped crack with the number of elements $M = 96$ (left) and $M = 2400$ (right).**Fig. 5.** Contour plots of the crack opening displacement (left) and stress intensity factor along the crack front (right) using the BEM model with $M = 2400$.

observed. Results of the normalized SIF values ($K_I / [2\sigma_{\infty} \sqrt{\pi a} / \pi]$) at location $(a, 0, 0)$ and for different BEM models are shown in Fig. 7. Again, good agreement between the BEM and analytical solutions are observed. The SIF results converge to within 2% of the analytical solution very quickly (at $M = 864$) and then improve very slowly afterwards. The BEM result with the finest mesh ($M = 4704$) still has a relative error of 1.66%. Considering the fact that constant elements are used here and no special treatment of the crack tip singularity (e.g., using quarter-point elements or crack edge elements [10]) is applied, the SIF results obtained are quite satisfactory.

This example shows that the BEM with constant elements can be applied to solve 3-D crack problems with satisfactory results, as have been done in the DDM research for decades. Better BEM/DDM results can be obtained if the analytical integration results are applied to compute all the integrals and fine meshes are used in the discretization.

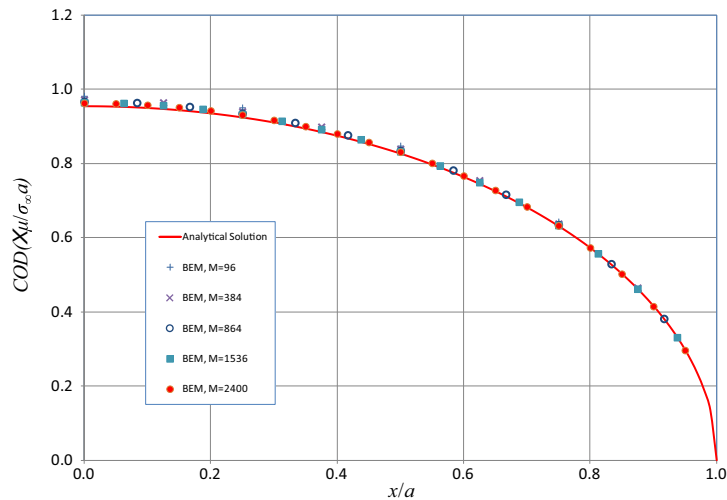


Fig. 6. Plot of the COD along the x -axis for models with different number of elements.

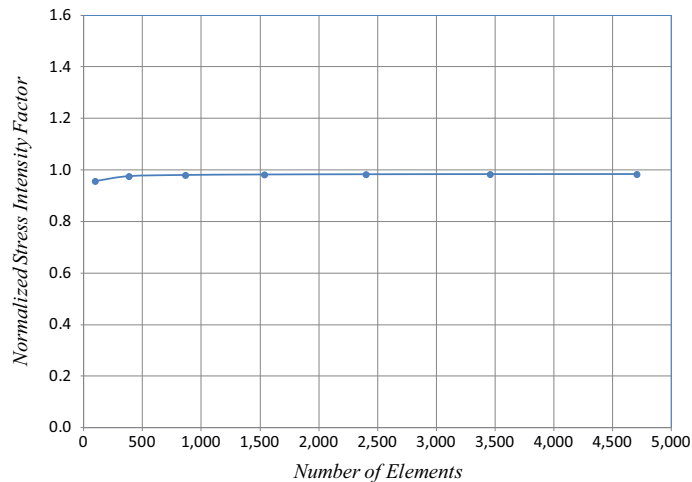


Fig. 7. Plot of the SIF using models with different number of elements.

5. Discussions

In this paper, the equivalence of the DDM equations and those from the BEM with constant elements for solving 3-D crack problems is established explicitly based on discretizing the displacement and traction BIEs. Therefore, the DDM and BEM are the same numerical method for solving the crack problems. More compact equations in tensor notations of the DDM equations are also found through these derivations (Eqs. (19) and (24)).

The DDM equations are discretized equations from the beginning and are formulated in local coordinate systems on the flat elements. Additional transformations are needed to apply the DDM to model cracks with curved surfaces or cracks in different orientations. On the other hand, the BEM is established based on the BIEs and is applicable to more general settings, regarding the crack geometries, orientations and the boundary conditions. Therefore, it might be advantageous to apply the BIE in formulating the numerical method (either DDM or BEM) directly, and also apply all the available results in the BEM research on the analytical integration and fast solution methods.

This equivalence or connection of the DDM and BEM suggests that the BEM based on the traction BIE has been applied in solving crack problems for four decades (since 1976 [1]), albeit in the name of the DDM. This is about one decade earlier than the commonly acknowledged time when the BEM using traction BIE was first introduced in solving crack problems. The equivalence of the DDM and BEM also indicates that the BEM with constant elements can be applied to solve crack problems successfully. The examples given in this paper using analytical integration and refined mesh further support this assertion. On the other hand, large-scale BEM models of cracks can be solved more efficiently if constant elements are used for which

analytical integration results are available, especially when the fast solution methods (FMM and ACA) are used. With the help of the fast solution methods for the BEM or DDM, the use of large numbers of elements in modeling crack problems should no longer be a barrier for the two methods. Large-scale BEM models with a few million elements can now be solved routinely on current desktop workstations [56].

Research on the BEM or DDM with constant elements and accelerated by the FMM and ACA for solving large-scale general 3-D crack problems is underway and will be reported in subsequent papers.

Acknowledgment

The author would like to acknowledge the funding support of the National Natural Science Foundation of China (Project No. 11472218) through Northwestern Polytechnical University for his research conducted there in the summer of 2015.

References

- [1] Crouch SL. Solution of plane elasticity problems by the displacement discontinuity method. *Int J Numer Meth Eng* 1976;10:301–43.
- [2] Crouch SL, Starfield AM. Boundary element methods in solid mechanics. London: George Allen & Unwin; 1983.
- [3] Bhattacharyya PK, Willment T. Quadratic approximations in the displacement discontinuity method. *Eng Anal* 1988;5:28–35.
- [4] Chan HCM, Li V, Einstein HH. A hybridized displacement discontinuity and indirect boundary element method to model fracture propagation. *Int J Fract* 1990;45:263–82.
- [5] Pan E. Dislocation in an infinite poroelastic medium. *Acta Mech* 1991;87:105–15.
- [6] Kuriyama K, Mizuta Y. Three-dimensional elastic analysis by the displacement discontinuity method with boundary division into triangular leaf elements. *Int J Rock Mech Min Sci Geomech Abstr* 1993;30:111–23.
- [7] Wen P, Fan T. The discontinuity displacement method applied to three-dimensional co-planar crack problem for any boundary value condition. *Eng Fract Mech* 1994;48:691–702.
- [8] Zhao M, Liu Y, Cheng C. Boundary-integral equations and the boundary-element method for three-dimensional fracture mechanics. *Eng Anal Boundary Elem* 1994;13:333–8.
- [9] Cheng AHD, Detournay E. On singular integral equations and fundamental solutions of poroelasticity. *Int J Solids Struct* 1998;35:4521–55.
- [10] Li H, Liu CL, Mizuta Y, Kayupov MA. Crack edge element of three-dimensional displacement discontinuity method with boundary division into triangular leaf elements. *Commun Numer Methods Eng* 2001;17:365–78.
- [11] Dong CY, de Pater CJ. Numerical implementation of displacement discontinuity method and its application in hydraulic fracturing. *Comput Methods Appl Mech Eng* 2001;191:745–60.
- [12] Shi J, Shen B, Stephansson O, Rinne M. A three-dimensional crack growth simulator with displacement discontinuity method. *Eng Anal Boundary Elem* 2014;48:73–86.
- [13] Jing L. A review of techniques, advances and outstanding issues in numerical modelling for rock mechanics and rock engineering. *Int J Rock Mech Min Sci* 2003;40:283–353.
- [14] Jo H, Hurt R. Testing and review of various displacement discontinuity elements for LEM crack problems. In: Bunger AP, McLennan J, Jeffrey R, editors. *Effective and sustainable hydraulic fracturing*. InTech; 2013.
- [15] Sheibani F. Solving three dimensional problems in natural and hydraulic fracture development: insight from displacement discontinuity modeling. Dissertation. Austin: Department of Petroleum and Geosystems Engineering, The University of Texas; 2013.
- [16] Sheibani F, Olson J. Stress intensity factor determination for three-dimensional crack using the displacement discontinuity method with applications to hydraulic fracture height growth and non-planar propagation paths. In: ISRM international conference for effective and sustainable hydraulic fracturing. InTech; 2013. p. 741–70.
- [17] Morris JP, Blair SC. Efficient displacement discontinuity method using fast multipole techniques. In: *Proceedings of the 4th North American rock mechanics symposium*. Seattle, WA: American Rock Mechanics Association; 2000.
- [18] Verde A, Ghassemi A. Efficient solution of large-scale displacement discontinuity problems using the fast multipole method. In: *Proceedings of the 47th US rock mechanics/geomechanics symposium*. San Francisco, CA: American Rock Mechanics Association; 2013.
- [19] Verde A, Ghassemi A. Fast multipole displacement discontinuity method (FM-DDM) for geomechanics reservoir simulations. *Int J Numer Anal Meth Geomech* 2015;39:1953–74.
- [20] Rizzo FJ. An integral equation approach to boundary value problems of classical elastostatics. *Quart. Appl. Math.* 1967;25:83–95.
- [21] Mukherjee S. *Boundary element methods in creep and fracture*. New York: Applied Science Publishers; 1982.
- [22] Cruse TA. *Boundary element analysis in computational fracture mechanics*. Dordrecht, The Netherlands: Kluwer Academic Publishers; 1988.
- [23] Cruse TA. BIE fracture mechanics analysis: 25 years of developments. *Comput Mech* 1996;18:1–11.
- [24] Blandford GE, Ingraffea AR, Liggett JA. Two-dimensional stress intensity factor computations using the boundary element method. *Int J Numer Meth Eng* 1981;17:387–404.
- [25] Hong HK, Chen JT. Derivations of integral equations of elasticity. *J Eng Mech* 1988;114:1028–44.
- [26] Gray LJ. Boundary element method for regions with thin internal cavities. *Eng Anal Boundary Elem* 1989;6:180–4.
- [27] Aliabadi MH. Boundary element formulations in fracture mechanics. *Appl Mech Rev* 1997;50:83–96.
- [28] Chen JT, Hong HK. Review of dual boundary element methods with emphasis on hypersingular integrals and divergent series. *Appl Mech Rev* 1999;52:17–33.
- [29] Aliabadi MH. *The boundary element method – applications in solids and structures*. Chichester: Wiley; 2002.
- [30] Martin PA, Rizzo FJ. On the boundary integral equations for crack problems. *Proc Roy Soc Lond A* 1989;421:341–55.
- [31] Krishnasamy G, Rudolph TJ, Schmerr LW, Rizzo FJ. Hypersingular boundary integral equations: some applications in acoustic and elastic wave scattering. *J Appl Mech* 1990;57:404–14.
- [32] Krishnasamy G, Rizzo FJ, Liu YJ. Scattering of acoustic and elastic waves by crack-like objects: the role of hypersingular integral equations. In: Thompson DO, Chimenti DE, editors. *Review of progress in quantitative nondestructive evaluation*. Brunswick, Maine: Plenum Press; 1991.
- [33] Krishnasamy G, Rizzo FJ, Rudolph TJ. Hypersingular boundary integral equations: their occurrence, interpretation, regularization and computation. In: Banerjee PK et al., editors. *Developments in boundary element methods*. London: Elsevier Applied Science Publishers; 1991.
- [34] Krishnasamy G, Rizzo FJ, Liu YJ. Some advances in boundary integral methods for wave-scattering from cracks. *Acta Mech* 1992;3(Suppl.):55–65.
- [35] Portela A, Aliabadi MH, Rooke DP. The dual boundary element method: effective implementation for crack problems. *Int J Numer Meth Eng* 1992;33:1269–87.
- [36] Krishnasamy G, Rizzo FJ, Liu YJ. Boundary integral equations for thin bodies. *Int J Numer Meth Eng* 1994;37:107–21.
- [37] Liu YJ, Rizzo FJ. Scattering of elastic waves from thin shapes in three dimensions using the composite boundary integral equation formulation. *J Acoust Soc Am* 1997;102(2):926–32.
- [38] Fukui T. Research on the boundary element method - development and applications of fast and accurate computations Ph.D. dissertation. Department of Global Environment Engineering, Kyoto University; 1998 [in Japanese].

- [39] Yoshida K. Applications of fast multipole method to boundary integral equation method Ph.D. dissertation. Department of Global Environment Engineering, Kyoto University; 2001.
- [40] Yoshida K, Nishimura N, Kobayashi S. Application of fast multipole Galerkin boundary integral equation method to crack problems in 3D. *Int J Numer Meth Eng* 2001;50:525–47.
- [41] Yoshida K, Nishimura N, Kobayashi S. Application of new fast multipole boundary integral equation method to elastostatic crack problems in three dimensions. *JSCE J Struct Eng* 2001;47A:169–79.
- [42] Guo Z, Liu YJ, Ma H, Huang S. A fast multipole boundary element method for modeling 2-D multiple crack problems with constant elements. *Eng Anal Boundary Elem* 2014;47:1–9.
- [43] Nikolskiy DV, Mogilevskaya SG, Labuz JF. Complex variables boundary element analysis of three-dimensional crack problems. *Eng Anal Boundary Elem* 2013;37:1532–44.
- [44] Mogilevskaya SG, Nikolskiy DV. The use of complex integral representations for analytical evaluation of three-dimensional BEM integrals – potential and elasticity problems. *Quart J Mech Appl Math* 2014;67:505–23.
- [45] Nikolskiy DV, Mogilevskaya SG, Labuz JF. Boundary element analysis of non-planar three-dimensional cracks using complex variables. *Int J Rock Mech Min Sci* 2015;76:44–54.
- [46] Rokhlin V. Rapid solution of integral equations of classical potential theory. *J Comput Phys* 1985;60:187–207.
- [47] Greengard LF. The rapid evaluation of potential fields in particle systems. Cambridge: The MIT Press; 1988.
- [48] Nishimura N. Fast multipole accelerated boundary integral equation methods. *Appl Mech Rev* 2002;55:299–324.
- [49] Liu YJ. Fast multipole boundary element method – theory and applications in engineering. Cambridge: Cambridge University Press; 2009.
- [50] Rjasanow S, Steinbach O. The fast solution of boundary integral equations. Berlin: Springer; 2007.
- [51] Bebendorf M. Hierarchical matrices: a means to efficiently solve elliptic boundary value problems. Berlin: Springer-Verlag; 2008.
- [52] Wang P, Yao Z. Fast multipole DBEM analysis of fatigue crack growth. *Comput Mech* 2006;38:223–33.
- [53] Wang HT, Yao ZH. A fast multipole dual boundary element method for the three-dimensional crack problems. *CMES: Comput Model Eng Sci* 2011;72:115–48.
- [54] Weber W, Kolk K, Kuhn G. Acceleration of 3D crack propagation simulation by the utilization of fast BEM-techniques. *Eng Anal Boundary Elem* 2009;33:1005–15.
- [55] Benedetti I, Aliabadi MH. A fast hierarchical dual boundary element method for three-dimensional elastodynamic crack problems. *Int J Numer Meth Eng* 2010;84:1038–67.
- [56] Liu YJ, Mukherjee S, Nishimura N, Schanz M, Ye W, Sutradhar A, et al. Recent advances and emerging applications of the boundary element method. *Appl Mech Rev* 2011;64:1–38.
- [57] Hong HK, Chen JT. Generality and special cases of dual integral equations of elasticity. *J Chinese Soc Mech Eng* 1988;9:1–9.
- [58] Linkov AM, Mogilevskaya SG. Hypersingular integrals in plane problems of the theory of elasticity. *PMM USSR* 1990;54:93–9.
- [59] Linkov AM, Mogilevskaya SG. Complex hypersingular BEM in plane elasticity problems. In: Sladek V, Sladek J, editors. *Singular integrals in boundary element method*. Southampton: Computational Mechanics Publications; 1998. p. 299–364.
- [60] Lin'kov AM, Mogilevskaya SG. Finite-part integrals in problems of three-dimensional cracks. *J Appl Math Mech* 1986;50:652–8.
- [61] Liu YJ, Li YX. Revisit of the equivalence of the displacement discontinuity method and boundary element method for solving crack problems. *Eng Anal Boundary Elem* 2014;47:64–7.
- [62] Mogilevskaya SG. Lost in translation: crack problems in different languages. *Int J Solids Struct* 2014;51:4492–503.
- [63] Brebbia CA, Dominguez J. *Boundary elements – an introductory course*. New York: McGraw-Hill; 1989.
- [64] Banerjee PK. *The boundary element methods in engineering*. 2nd ed. New York: McGraw-Hill; 1994.
- [65] Bonnet M. *Boundary integral equation methods for solids and fluids*. Chichester: John Wiley & Sons; 1995.
- [66] Liu YJ. Analysis of shell-like structures by the boundary element method based on 3-D elasticity: formulation and verification. *Int J Numer Meth Eng* 1998;41:541–58.
- [67] Davey K, Hinduja S. Analytical integration of linear three-dimensional triangular elements in BEM. *Appl Math Model* 1989;13:450–61.
- [68] Salvadori A. Analytical integrations of hypersingular kernel in 3D BEM problems. *Comput Methods Appl Mech Eng* 2001;190:3957–75.
- [69] Carini A, Salvadori A. Analytical integrations 3D BEM. *Comput Mech* 2002;28:177–85.
- [70] Salvadori A. Analytical integrations in 3D BEM for elliptic problems: evaluation and implementation. *Int J Numer Meth Eng* 2010;84:505–42.
- [71] Liu YJ, Nishimura N, Otani Y. Large-scale modeling of carbon-nanotube composites by the boundary element method based on a rigid-inclusion model. *Comput Mater Sci* 2005;34:173–87.
- [72] Liu YJ, Nishimura N, Otani Y, Takahashi T, Chen XL, Munakata H. A fast boundary element method for the analysis of fiber-reinforced composites based on a rigid-inclusion model. *J Appl Mech* 2005;72:115–28.
- [73] Liu YJ, Li YX. Slow convergence of the BEM with constant elements in solving beam bending problems. *Eng Anal Boundary Elem* 2014;39:1–4.
- [74] Bower AF. *Applied mechanics of solids*. Boca Raton: CRC Press; 2009.
- [75] Timoshenko SP, Goodier JN. *Theory of elasticity*. 3rd ed. New York: McGraw-Hill; 1987.
- [76] Liu YJ, Ye W, Deng Y. On the identities for elastostatic fundamental solution and nonuniqueness of the traction BIE solution for multi-connected domains. *ASME J Appl Mech* 2013;80:051012.
- [77] Green AE, Zerna W. *Theoretical elasticity*. 2nd ed. New York: Oxford University Press; 1968.
- [78] Anderson TL. *Fracture mechanics: fundamentals and applications*. 3rd ed. Boca Raton: CRC Press; 2005.